

非饱和土半空间 Lamb 问题及能量传输特性¹⁾周凤玺^{*,†,2)} 张雅森^{*} 曹小林^{**} 牟占霖^{*}^{*}(兰州理工大学土木工程学院, 兰州 730050)[†](西部土木工程防灾减灾教育部工程研究中心, 兰州 730050)^{**}(东南大学土木工程学院, 南京 211189)

摘要 地球表面绝大多数土层处于非饱和状态, 故采用传统饱和两相介质理论进行动力学分析时, 结果往往与实际不符. 针对这一问题, 本文以非饱和半空间作为研究对象, 基于连续介质力学和多孔介质理论, 考虑非饱和多孔介质中各相的质量守恒方程、动量守恒方程、本构方程以及有效应力原理等基本方程, 建立了以骨架位移、孔隙水压力和孔隙气压力为基本未知量的动力学控制方程. 针对非饱和半空间表面在竖向集中简谐荷载作用下的动力学响应及能量传输问题, 建立了频域内经典 Lamb 问题的轴对称计算模型, 采用 Helmholtz 分解法, 通过引入势函数 ϕ 和 ψ 表示骨架的位移分量, 结合本构方程获得了不同边界条件下半空间表面位移场和能量场等物理量的解析解答, 并通过数值算例对荷载参数(激振频率)、材料参数(饱和度、渗透系数)等影响因素进行了分析与讨论. 结果表明: (1) 饱和度的升高或者激振频率下降, 都会提高非饱和半空间的表面位移幅值; (2) 当渗透系数下降至一临界值时, 地表位移幅值会趋于一极限值, 并且透水(气)边界与不透水(气)边界条件下渗透系数的影响表现出明显的差异性.

关键词 非饱和半空间, Lamb 问题, 能量传输, 竖向集中简谐荷载, 解析解答

中图分类号: TU435 文献标识码: A doi: 10.6052/0459-1879-21-195

LAMB'S PROBLEM AND CHARACTERISTIC OF ENERGY TRANSMISSION IN UNSATURATED HALF-SPACE¹⁾Zhou Fengxi^{*,†,2)} Zhang Yasen^{*} Cao Xiaolin^{**} Mu Zhanlin^{*}^{*}(School of Civil Engineering, Lanzhou University of Technology, Lanzhou 730050, China)[†](Engineering Research Center of Disaster Mitigation in Civil Engineering of Ministry of education, Lanzhou 730050, China)^{**}(School of Civil Engineering, Southeast University, Nanjing 211189, China)

Abstract Because unsaturated soil is widely distributed on the earth's surface, when the traditional saturated two-phase medium theory is used for dynamic analysis, the results are often inconsistent with the actual situation. Aiming at this problem, this paper takes unsaturated elastic half-space as the research object, firstly based on continuum mechanics and porous media theory, and then considers the basic equations of mass conservation equation, momentum conservation equation, constitutive equation and effective stress principle of each phase in unsaturated porous media, and finally, we established a dynamic control equation in which skeleton displacement, pore water pressure and pore gas pressure are basically unknown quantities. Aiming at the dynamic response and energy transmission of the

2021-05-08 收稿, 2021-06-10 录用, 2021-06-13 网络版发表.

1) 国家自然科学基金(11962016, 51978320), 甘肃省基础研究创新群体项目(20JR5RA478)资助.

2) 周凤玺, 教授, 主要从事岩土力学、复合材料结构力学方面的研究工作. E-mail: zfx620@lut.edu.cn

引用格式: 周凤玺, 张雅森, 曹小林, 牟占霖. 非饱和土半空间 Lamb 问题及能量传输特性. 力学学报, 2021, 53(7): 2079-2089

Zhou Fengxi, Zhang Yasen, Cao Xiaolin, Mu Zhanlin. Lamb's problem and characteristic of energy transmission in unsaturated half-space. *Chinese Journal of Theoretical and Applied Mechanics*, 2021, 53(7): 2079-2089

unsaturated half-space surface under the action of vertical concentrated harmonic loads, an axisymmetric calculation model of the classical Lamb problem in the frequency domain is established. The Helmholtz decomposition method is used and the displacement component of the skeleton uses the potential function Φ and Ψ to represent, and combined with the constitutive equation, the analytical solutions of physical quantities such as the displacement field and energy field of the half-space surface under different boundary conditions are obtained. Finally, influencing factors such as load parameters (excitation frequency) and material parameters (saturation, permeability coefficient) are analyzed and discussed through numerical examples. The results show that: (1) An increase in saturation or a decrease in excitation frequency will increase the surface displacement amplitude of the unsaturated half-space; (2) When the permeability coefficient drops to a critical value, the surface displacement amplitude will tend to a limit value, and the influence of permeability coefficient under permeable (gas) boundary and impermeable (gas) boundary conditions shows obvious difference.

Key words unsaturated half space, Lamb's problem, energy transmission, vertical concentrated harmonic load, analytical solutions

引言

弹性半空间的波动响应一直是弹性动力学领域的研究热点, 其中 Lamb 问题最具代表性. 随着研究的深入, 不同集中荷载形式 (点源和线源、表面和内部等) 作用下单相弹性介质的 Lamb 问题已经取得了比较完备的体系. 近年来, 有关多相多孔介质的 Lamb 问题逐渐受到人们的重视. 自 Biot^[1-2] 建立了两相介质的波动方程后, 国内外学者针对饱和半空间 Lamb 问题已经取得了一系列研究成果, 主要包括荷载作用于半空间表面^[3-5] 和半空间内部^[6-9] 以及层状地基^[10-14] 等不同方面的动力响应研究. 相对于饱和土, 在工程建设中大量涉及到的是处于地下水位以上的非饱和土体, 而已有研究表明, 介质中孔隙气体的存在对其动力响应行为、弹性波传播特性以及能量传输产生巨大影响, 因此研究非饱和半空间的动力学行为在岩土工程、地震工程等领域有着重要的理论和应用价值.

由于非饱和多孔介质物理力学特性的复杂性, 使得对非饱和半空间 Lamb 问题及能量传输特性的研究成果较少. 王春玲等^[15-17] 采用积分变换法和消元法求得了非饱和地基受竖向简谐荷载作用下的稳态响应积分变换解, 但其最终解的形式十分复杂, 不便于应用. 徐明江等^[18-20] 以三相多孔介质模型为基础, 通过引入双变量本构关系, 采用解析法研究了简谐荷载作用下非饱和土地基的动力响应问题, 给出了积分形式的解答, 但并未考虑颗粒间吸应力对非饱和半空间动力学特征的影响. Zhang 等^[21] 在假定

土骨架为多孔弹性连续介质, 且具有均匀性和各向同性的基础上, 通过应用 Fourier 展开技术和 Hankel 积分的方法得到了在内部激励作用下的非饱和土中动态格林函数解, 但上述研究成果均未讨论不同边界条件对非饱和半空间表面的动力学响应特征及能量传输特性的影响规律.

本文在已有研究成果的基础之上, 考虑非饱和土中颗粒间吸应力的作用, 结合质量守恒方程、动量平衡方程及有效应力原理等基本方程, 运用 Helmholtz 分解法, 在柱坐标系下建立了非饱和半空间的动力学控制方程. 分别考虑透水 (气) 和不透水 (气) 两种边界条件, 对频域内的轴对称问题进行求解, 得到了非饱和半空间表面受到竖向集中简谐荷载作用下的解析解答, 并且通过参数分析讨论了在不同饱和度、不同振动频率以及不同渗透系数下的动力响应特性和能量传输的变化及其影响规律, 以期为不同边界条件下非饱和半空间的表面振动问题提供参考依据.

1 基本方程

如图 1 所示的非饱和半空间表面受到频率为 ω , 幅度为 q_0 的垂直简谐荷载作用, 考虑轴对称性, 问题的基本方程包括如下 6 类.

(1) 时域内固体骨架动量平衡方程

$$\frac{\partial \sigma_r}{\partial r} + \frac{\partial \tau_{rz}}{\partial z} + \frac{1}{r}(\sigma_r - \sigma_\theta) = \bar{\rho}_s \ddot{u}_r + \bar{\rho}_1 \ddot{w}_r + \bar{\rho}_a \ddot{v}_r \quad (1a)$$

$$\frac{\partial \tau_{rz}}{\partial r} + \frac{\partial \sigma_z}{\partial z} + \frac{1}{r} \tau_{rz} = \bar{\rho}_s \ddot{u}_z + \bar{\rho}_1 \ddot{w}_z + \bar{\rho}_a \ddot{v}_z \quad (1b)$$

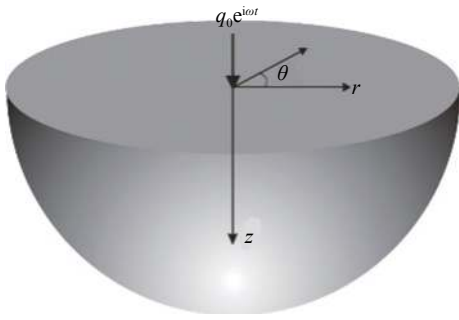


图 1 半空间计算模型

Fig. 1 Half-space calculation mode

(2) 时域内孔隙流体运动平衡方程

$$-\frac{\partial p_l}{\partial r} = b^l (\dot{w}_r - \dot{u}_r) + \rho_l \ddot{w}_r \quad (2a)$$

$$-\frac{\partial p_l}{\partial z} = b^l (\dot{w}_z - \dot{u}_z) + \rho_l \ddot{w}_z \quad (2b)$$

$$-\frac{\partial p_a}{\partial r} = b^a (\dot{v}_r - \dot{u}_r) + \rho_a \ddot{v}_r \quad (2c)$$

$$-\frac{\partial p_a}{\partial z} = b^a (\dot{v}_z - \dot{u}_z) + \rho_a \ddot{v}_z \quad (2d)$$

式 (1) 和式 (2) 中, $\sigma_r, \sigma_\theta, \sigma_z, \tau_{rz}$ 分别为代表单元体上的总应力和剪应力; u_r, u_θ, u_z 分别为径向位移、环向位移和竖向位移; w_r, w_θ, w_z 分别为孔隙中液体的径向位移、环向位移和竖向位移; v_r, v_θ, v_z 分别为孔隙中气体的径向位移、环向位移和竖向位移; p_l 和 p_a 分别为孔隙水压力和孔隙气压力; $\bar{\rho}_s, \bar{\rho}_l$ 和 $\bar{\rho}_a$ 分别为固相、液相和气相的表观密度。

考虑孔隙中的流体渗透形式符合达西定律, 用固有渗透系数 K 表征气相和液相的渗透系数 k_l 和 k_a 分别为

$$k_l = \frac{\rho_l g}{\eta_l} K \quad (3a)$$

$$k_a = \frac{\rho_a g}{\eta_a} K \quad (3b)$$

则式 (2a)~式 (2d) 中系数 b^l 和 b^a 可表示为如下形式

$$b^l = \frac{n S_r \eta_l}{K} \quad (4a)$$

$$b^a = \frac{n(1-S_r)\eta_a}{K} \quad (4b)$$

式中, n 为孔隙率; S_r 为饱和度; g 为重力加速度; η_l 和 η_a 分别为液相和气相的动力黏度系数。

(3) 有效应力原理

有效应力原理是土力学的核心, 目前关于非饱和土中有效应力原理大致可分为单变量理论^[22]、双变量理论^[23]和复合变量理论^[24]。其中, Lu 等^[25]在考虑微观颗粒间作用力和有效应力的基础上提出了吸应力表示的有效应力公式

$$\sigma'_{ij} = (\sigma_{ij} - p_a \delta_{ij}) - \sigma_s \delta_{ij} \quad (5)$$

式中, $\sigma_s = -(p_a - p_l) S_e$ 表示粒间吸应力, S_e 为有效饱和度, $S_e = (S_r - S_{w0}) / (1 - S_{w0})$, S_{w0} 为残余饱和度。吸应力表示的有效应力公式是非饱和介质中两相流体压力的函数, 主要受饱和度变化的影响, 消除了 Bishop 有效应力原理中对参数 χ 的依赖性。

(4) 质量守恒方程

忽略各相之间的质量交换, 非饱和多孔介质各相的质量守恒方程可描述为^[26-28]

$$\partial \bar{\rho}_m / \partial t + (\bar{\rho}_m \dot{u}_i^m)_{,i} = 0, \quad m = s, l, a \quad (6)$$

式中, $\bar{\rho}_m$ 为非饱和半空间中各相介质的表观密度; \dot{u}_i^m 为非饱和半空间中各相介质在不同方向上位移的时间导数。

(5) 本构方程

考虑固相颗粒的可压缩性, 弹性各向同性非饱和介质的本构方程为

$$\sigma_r = (\lambda + 2\mu) \frac{\partial u_r}{\partial r} + \lambda \frac{u_r}{r} + \lambda \frac{\partial u_z}{\partial z} - \alpha S_e p_l - \alpha (1 - S_e) p_a \quad (7a)$$

$$\sigma_\theta = \lambda \frac{\partial u_r}{\partial r} + (\lambda + 2\mu) \frac{u_r}{r} + \lambda \frac{\partial u_z}{\partial z} - \alpha S_e p_l - \alpha (1 - S_e) p_a \quad (7b)$$

$$\sigma_z = \lambda \frac{\partial u_r}{\partial r} + \lambda \frac{u_r}{r} + (\lambda + 2\mu) \frac{\partial u_z}{\partial z} - \alpha S_e p_l - \alpha (1 - S_e) p_a \quad (7c)$$

$$\tau_{rz} = \mu \left(\frac{\partial u_r}{\partial z} + \frac{\partial u_z}{\partial r} \right) \quad (7d)$$

式中, $\alpha = 1 - K_b / K_s$, K_s 和 K_b 分别为固相颗粒以及骨架的体积压缩模量; λ 和 μ 为 Lamé 常数。

(6) 渗流连续方程

$$-\dot{p}_l = a_{11} \left(\frac{\partial \dot{u}_r}{\partial r} + \frac{\dot{u}_r}{r} + \frac{\partial \dot{u}_z}{\partial z} \right) + a_{12} \left(\frac{\partial \dot{w}_r}{\partial r} + \frac{\dot{w}_r}{r} + \frac{\partial \dot{w}_z}{\partial z} \right) + a_{13} \left(\frac{\partial \dot{v}_r}{\partial r} + \frac{\dot{v}_r}{r} + \frac{\partial \dot{v}_z}{\partial z} \right) \quad (8a)$$

$$-\dot{p}_a = a_{21} \left(\frac{\partial \dot{u}_r}{\partial r} + \frac{\dot{u}_r}{r} + \frac{\partial \dot{u}_z}{\partial z} \right) + a_{22} \left(\frac{\partial \dot{w}_r}{\partial r} + \frac{\dot{w}_r}{r} + \frac{\partial \dot{w}_z}{\partial z} \right) + a_{23} \left(\frac{\partial \dot{v}_r}{\partial r} + \frac{\dot{v}_r}{r} + \frac{\partial \dot{v}_z}{\partial z} \right) \quad (8b)$$

式中, 系数 a_{ij} 的具体表达式详见附录 A. 本构方程 (7) 和渗流连续方程 (8) 的具体推导过程分别见附录 B 和附录 C.

2 问题的求解

2.1 控制方程

考虑简谐荷载作用下各位移分量的形式如下

$$u_r = u_r(r, \theta, z, \omega) e^{i\omega t} \quad (9a)$$

$$u_z = u_z(r, \theta, z, \omega) e^{i\omega t} \quad (9b)$$

$$w_r = w_r(r, \theta, z, \omega) e^{i\omega t} \quad (9c)$$

$$w_z = w_z(r, \theta, z, \omega) e^{i\omega t} \quad (9d)$$

$$v_r = v_r(r, \theta, z, \omega) e^{i\omega t} \quad (9e)$$

$$v_z = v_z(r, \theta, z, \omega) e^{i\omega t} \quad (9f)$$

将式 (9) 代入孔隙流体运动平衡方程 (2) 中, 并结合式 (1)、式 (7) 和式 (8), 整理后可得频域内非饱和半空间的动力控制方程

$$V_P^2 \frac{\partial}{\partial r} \left(\frac{\partial u_r}{\partial r} + \frac{u_r}{r} + \frac{\partial u_z}{\partial z} \right) + V_S^2 \frac{\partial}{\partial z} \left(\frac{\partial u_r}{\partial z} - \frac{\partial u_z}{\partial r} \right) + \kappa_1 \omega^2 u_r - \kappa_2 \frac{\partial p_l}{\partial r} - \kappa_3 \frac{\partial p_a}{\partial r} = 0 \quad (10a)$$

$$V_P^2 \frac{\partial}{\partial z} \left(\frac{\partial u_r}{\partial r} + \frac{u_r}{r} + \frac{\partial u_z}{\partial z} \right) + V_S^2 \frac{\partial}{\partial r} \left(\frac{\partial u_z}{\partial r} - \frac{\partial u_r}{\partial z} \right) + \kappa_1 \omega^2 u_z - \kappa_2 \frac{\partial p_l}{\partial z} - \kappa_3 \frac{\partial p_a}{\partial z} + \frac{V_S^2}{r} \left(\frac{\partial u_z}{\partial r} - \frac{\partial u_r}{\partial z} \right) = 0 \quad (10b)$$

$$-p_l = \left(a_{11} + a_{12} \frac{b^l i \omega}{\theta_1} + a_{13} \frac{b^a i \omega}{\theta_2} \right) \left(\frac{\partial u_r}{\partial r} + \frac{u_r}{r} + \frac{\partial u_z}{\partial z} \right) - \frac{a_{12}}{\theta_1} \nabla^2 p_l - \frac{a_{13}}{\theta_2} \nabla^2 p_a \quad (11a)$$

$$l - p_a = \left(a_{21} + a_{22} \frac{b^l i \omega}{\theta_1} + a_{23} \frac{b^a i \omega}{\theta_2} \right) \left(\frac{\partial u_r}{\partial r} + \frac{u_r}{r} + \frac{\partial u_z}{\partial z} \right) - \frac{a_{22}}{\theta_1} \nabla^2 p_l - \frac{a_{23}}{\theta_2} \nabla^2 p_a \quad (11b)$$

式中 $\theta_1 = b^l i \omega - \rho_l \omega^2$, $\theta_2 = b^a i \omega - \rho_a \omega^2$, $\kappa_1 = 1 + \frac{\bar{\rho}_1 b^l i \omega}{\bar{\rho}_s \theta_1} +$

$\frac{\bar{\rho}_a b^a i \omega}{\bar{\rho}_s \theta_2}$, $\kappa_2 = \frac{\bar{\rho}_1 \omega^2}{\bar{\rho}_s \theta_1} + \frac{\alpha S_e}{\bar{\rho}_s}$, $\kappa_3 = \frac{\bar{\rho}_a \omega^2}{\bar{\rho}_s \theta_2} + \frac{\alpha(1 - S_e)}{\bar{\rho}_s}$, $V_P = \sqrt{(\lambda + 2\mu)/\bar{\rho}_s}$ 为纵波波速, $V_S = \sqrt{\mu/\bar{\rho}_s}$ 为横波波速.

根据 Helmholtz 分解定理, 引入柱坐标系下的两个势函数 Φ 和 Ψ 表示 u_r 和 u_z 如下

$$u_r = \frac{\partial \Phi}{\partial r} + \frac{\partial^2 \Psi}{\partial r \partial z} \quad (12a)$$

$$u_z = \frac{\partial \Phi}{\partial z} - \frac{\partial \Psi}{r \partial r} - \frac{\partial^2 \Psi}{\partial r^2} \quad (12b)$$

将式 (12a) 分别代入式 (10a) 和式 (11) 中, 可得

$$V_P^2 \nabla^2 \Phi + \kappa_1 \omega^2 \Phi = \kappa_2 p_l + \kappa_3 p_a \quad (13)$$

$$V_S^2 \nabla^2 \Psi + \kappa_1 \omega^2 \Psi = 0 \quad (14)$$

$$-p_l = \left(a_{11} + a_{12} \frac{b^l i \omega}{\theta_1} + a_{13} \frac{b^a i \omega}{\theta_2} \right) \nabla^2 \Phi - \frac{a_{12}}{\theta_1} \nabla^2 p_l - \frac{a_{13}}{\theta_2} \nabla^2 p_a \quad (15a)$$

$$-p_a = \left(a_{21} + a_{22} \frac{b^l i \omega}{\theta_1} + a_{23} \frac{b^a i \omega}{\theta_2} \right) \nabla^2 \Phi - \frac{a_{22}}{\theta_1} \nabla^2 p_l - \frac{a_{23}}{\theta_2} \nabla^2 p_a \quad (15b)$$

考虑到因变量的时间导数同二阶空间导数的乘积与其时间导数同一阶空间导数的乘积相比, 前者是高阶小量^[21]. 因此, 利用式 (8) 可以得到

$$p_a = \frac{a_{21} + a_{22} \frac{b^l i \omega}{\theta_1} + a_{23} \frac{b^a i \omega}{\theta_2}}{a_{11} + a_{12} \frac{b^l i \omega}{\theta_1} + a_{13} \frac{b^a i \omega}{\theta_2}} p_l \quad (16a)$$

$$p_l = \frac{a_{11} + a_{12} \frac{b^l i \omega}{\theta_1} + a_{13} \frac{b^a i \omega}{\theta_2}}{a_{21} + a_{22} \frac{b^l i \omega}{\theta_1} + a_{23} \frac{b^a i \omega}{\theta_2}} p_a \quad (16b)$$

将式 (16) 代入式 (13), 可得

$$p_l = \frac{V_P^2}{h_1} \nabla^2 \Phi + \frac{\kappa_1 \omega^2}{h_1} \Phi \quad (17a)$$

$$p_a = \frac{V_P^2}{h_2} \nabla^2 \Phi + \frac{\kappa_1 \omega^2}{h_2} \Phi \quad (17b)$$

将式 (17) 代入式 (15), 整理后可得

$$\nabla^2 (\nabla^2 \Phi) + \frac{H_2}{H_1} \nabla^2 \Phi + \frac{H_3}{H_1} \Phi = 0 \quad (18)$$

式中

$$\begin{aligned}
 H_1 &= \frac{a_{22} - a_{12}}{\theta_1} \frac{V_P^2}{h_1} + \frac{a_{23} - a_{13}}{\theta_2} \frac{V_P^2}{h_2} \\
 H_2 &= \frac{a_{22} - a_{12}}{\theta_1} \frac{\kappa_1 \omega^2}{h_1} + \frac{a_{23} - a_{13}}{\theta_2} \frac{\kappa_1 \omega^2}{h_2} + a_{21} - a_{11} + \\
 &\quad (a_{22} - a_{12}) \frac{b^1 i \omega}{\theta_1} + (a_{23} - a_{13}) \frac{b^2 i \omega}{\theta_2} + \frac{V_P^2}{h_1} - \frac{V_P^2}{h_2} \\
 H_3 &= \frac{\kappa_1 \omega^2}{h_1} - \frac{\kappa_1 \omega^2}{h_2} \\
 h_1 &= \kappa_2 + \kappa_3 - \frac{a_{21} + a_{22} \frac{b^1 i \omega}{\theta_1} + a_{23} \frac{b^2 i \omega}{\theta_2}}{a_{11} + a_{12} \frac{b^1 i \omega}{\theta_1} + a_{13} \frac{b^2 i \omega}{\theta_2}} \\
 h_2 &= \kappa_2 - \frac{a_{11} + a_{12} \frac{b^1 i \omega}{\theta_1} + a_{13} \frac{b^2 i \omega}{\theta_2}}{a_{21} + a_{22} \frac{b^1 i \omega}{\theta_1} + a_{23} \frac{b^2 i \omega}{\theta_2}} + \kappa_3
 \end{aligned}$$

方程 (14) 和方程 (18) 即为以势函数表示的频域内控制方程. 在得到势函数解答的基础上, 可通过基本方程得到各位移分量、应力分量等物理量的解答.

2.2 解析解答

利用分离变量法求解微分方程 (14) 和 (18), 可得

$$\Phi_{11} = [A_{11} I_0(\zeta_{11} r) + B_{11} K_0(\zeta_{11} r)] \cdot [C_{11} \sin(mz) + D_{11} \cos(mz)] e^{i\omega t} \quad (19a)$$

$$\Phi_{12} = [A_{12} I_0(\zeta_{12} r) + B_{12} K_0(\zeta_{12} r)] \cdot [C_{12} \sin(mz) + D_{12} \cos(mz)] e^{i\omega t} \quad (19b)$$

$$\Psi = [A_2 I_0(\zeta_2 r) + B_2 K_0(\zeta_2 r)] \cdot [C_2 \sin(mz) + D_2 \cos(mz)] e^{i\omega t} \quad (20)$$

式中, $I_0(\zeta_{11} r)$, $K_0(\zeta_{11} r)$, $I_0(\zeta_{12} r)$, $K_0(\zeta_{12} r)$, $I_0(\zeta_2 r)$, $K_0(\zeta_2 r)$ 分别为第一类和第二类零阶贝塞尔函数;

$$\begin{aligned}
 d_{11} &= \frac{H_2}{H_1}, \quad d_{12} = \frac{H_3}{H_1}, \quad \xi_2 = \sqrt{-\frac{\kappa_1 \omega^2}{V_S^2}} \\
 \xi_{11}^2 &= \frac{-d_{11} + \sqrt{d_{11}^2 - 4d_{12}}}{2}, \quad \xi_{12}^2 = \frac{-d_{11} - \sqrt{d_{11}^2 - 4d_{12}}}{2} \\
 \zeta_{11} &= \sqrt{\xi_{11}^2 + m}, \quad \zeta_{12} = \sqrt{\xi_{12}^2 + m}, \quad \zeta_2 = \sqrt{\xi_2^2 + m}
 \end{aligned}$$

待定系数 A, B, C, D 由具体的边界条件确定.

考虑如下边界条件

$$\sigma_z \Big|_{z=0; 0 \leq r \leq r_0} = q_0 e^{i\omega t} \quad (21)$$

$$\tau_{rz} \Big|_{z=0} = 0 \quad (22)$$

$$u_r \Big|_{r,z \rightarrow \infty} = u_z \Big|_{r,z \rightarrow \infty} = 0 \quad (23)$$

根据边界条件 (21) ~ (23) 可得

$$A_{11} = A_{12} = A_2 = C_{11} = C_{12} = D_2 = 0 \quad (24)$$

$$m = \frac{(2\beta - 1)\pi}{2z}, \quad \beta = 1, 2, 3, \dots \quad (25)$$

因此, 对于势函数可重写成以下形式

$$\Phi_m = \cos(mz) [B_{11m} K_0(\zeta_{11m} r) + B_{12m} K_0(\zeta_{12m} r)] e^{i\omega t} \quad (26)$$

$$\Psi_m = \sin(mz) B_{2m} K_0(\zeta_{2m} r) e^{i\omega t} \quad (27)$$

将式 (26) 和式 (27) 代入式 (12) 和式 (17) 中, 最终可获得非饱和多孔介质中孔隙压力及位移分量的表达式为

$$p_{1m} = \sum_{\beta=1}^{\infty} \cos(mz) [B_{11m} K_0(\zeta_{11m} r) \zeta_{11m} + B_{12m} K_0(\zeta_{12m} r) \zeta_{12m}] \frac{e^{i\omega t}}{h_1} \quad (28a)$$

$$p_{2m} = \sum_{\beta=1}^{\infty} \cos(mz) [B_{11m} K_0(\zeta_{11m} r) \zeta_{11m} + B_{12m} K_0(\zeta_{12m} r) \zeta_{12m}] \frac{e^{i\omega t}}{h_2} \quad (28b)$$

$$u_r = -e^{i\omega t} \sum_{\beta=1}^{\infty} \cos(mz) [B_{11m} K_1(\zeta_{11m} r) \zeta_{11m} + B_{12m} K_1(\zeta_{12m} r) \zeta_{12m} + B_{2m} K_1(\zeta_{2m} r) m \zeta_{2m}] \quad (29a)$$

$$u_z = e^{i\omega t} \sum_{\beta=1}^{\infty} \sin(mz) [-B_{11m} K_0(\zeta_{11m} r) m - B_{12m} K_0(\zeta_{12m} r) m + B_{2m} K_0(\zeta_{2m} r) \zeta_{2m}^2] \quad (29b)$$

将孔隙压力和位移的结果代入本构方程 (7) 中, 可得各应力分量的表达式为

$$\begin{aligned}
 \sigma_r &= - \sum_{\beta=0}^{\infty} \cos(mz) \left\{ B_{11m} \left[\eta_{11m} K_0(\zeta_{11m} r) - \frac{2\mu \zeta_{11m}}{r} K_1(\zeta_{11m} r) \right] + \right. \\
 &\quad B_{12m} \left[\eta_{12m} K_0(\zeta_{12m} r) - \frac{2\mu \zeta_{12m}}{r} K_1(\zeta_{12m} r) \right] + \\
 &\quad \left. B_{2m} m \left[\eta_{2m} K_0(\zeta_{2m} r) - \frac{2\mu \zeta_{2m}}{r} K_1(\zeta_{2m} r) \right] \right\} e^{i\omega t} \quad (30a)
 \end{aligned}$$

$$\sigma_z = -e^{i\omega t} \sum_{\beta=0}^{\infty} \cos(mz) [B_{11m} \eta'_{11m} K_0(\zeta_{11m} r) + B_{12m} \eta'_{12m} K_0(\zeta_{12m} r) + B_{2m} \eta'_{2m} K_0(\zeta_{2m} r)] \quad (30b)$$

对于本文所讨论问题的描述, 在非饱和半空间表面 ($z = 0$) 分别考虑透水 (气) 和不透水 (气) 两种边界条件.

(1) 当半空间表面排水 (气) 时, 土体表面孔隙气压力和孔隙水压力为 0, 即

$$p|_{z=0} = p_a|_{z=0} = 0 \quad (31)$$

此时, 式 (28) ~ 式 (30) 中各参数分别为

$$B_{11m} = \frac{\delta_6}{\delta_6(\delta_1 + \delta_0\delta_2) - \delta_3(\delta_4 + \delta_0\delta_5)} \delta$$

$$B_{12m} = \frac{\delta_0\delta_6}{\delta_6(\delta_1 + \delta_0\delta_2) - \delta_3(\delta_4 + \delta_0\delta_5)} \delta$$

$$B_{2m} = \frac{\delta_4 + \delta_0\delta_5}{\delta_3(\delta_4 + \delta_0\delta_5) - \delta_6(\delta_1 + \delta_0\delta_2)} \delta$$

$$\delta = \frac{q_0}{\pi r_0^2}, \delta_0 = -\frac{K_0(\zeta_{11m} r)(\zeta_{11m}^2 + m^2)}{K_0(\zeta_{12m} r)(\zeta_{12m}^2 + m^2)}$$

$$\delta_1 = [(\lambda + 2\mu)m^2 + \lambda\zeta_{11m}^2] K_0(\zeta_{11m} r_0)$$

$$\delta_2 = [(\lambda + 2\mu)m^2 + \lambda\zeta_{12m}^2] K_0(\zeta_{12m} r_0)$$

$$\delta_3 = -2m\mu\zeta_{2m}^2 K_0(\zeta_{2m} r_0), \delta_4 = 2m\zeta_{11m} K_1(\zeta_{11m} r_0)$$

$$\delta_5 = 2m\zeta_{12m} K_1(\zeta_{12m} r_0), \delta_6 = (m^2 - \zeta_{2m}^2)\zeta_{2m} K_1(\zeta_{2m} r_0)$$

$$S_{11m} = \kappa_1 \omega^2 - V_p^2 (\zeta_{11m}^2 + m^2)$$

$$S_{12m} = \kappa_1 \omega^2 - V_p^2 (\zeta_{12m}^2 + m^2)$$

$$\eta_{11m} = (\lambda + 2\mu)\zeta_{11m}^2 + \lambda m^2 + \alpha S_e \frac{S_{11m}}{h_1} + \alpha(1 - S_e) \frac{S_{11m}}{h_2}$$

$$\eta_{12m} = (\lambda + 2\mu)\zeta_{12m}^2 + \lambda m^2 + \alpha S_e \frac{S_{12m}}{h_1} + \alpha(1 - S_e) \frac{S_{12m}}{h_2}$$

$$\eta_{2m} = (\lambda + 2\mu)\zeta_{2m}^2 - \lambda\zeta_{2m}$$

$$\eta'_{11m} = (\lambda + 2\mu)m^2 + \lambda\zeta_{11m}^2 + \alpha S_e \frac{S_{11m}}{h_1} + \alpha(1 - S_e) \frac{S_{11m}}{h_2}$$

$$\eta'_{12m} = (\lambda + 2\mu)m^2 + \lambda\zeta_{12m}^2 + \alpha S_e \frac{S_{12m}}{h_1} + \alpha(1 - S_e) \frac{S_{12m}}{h_2}$$

$$\eta'_{2m} = -2m\mu\zeta_{2m}^2$$

(2) 当半空间表面不排水 (气) 时, 土体表面孔隙流体和土骨架之间的相对位移为 0, 即

$$\mathbf{u} = \mathbf{w} = \mathbf{v} \quad (32)$$

此时孔隙中流体和土骨架间的位移关系由式 (2) 得

$$\mathbf{u} = \mathbf{w} = \frac{i\omega b^1 \mathbf{u} - \nabla p_1}{\theta_1} \quad (33a)$$

$$\mathbf{u} = \mathbf{v} = \frac{i\omega b^a \mathbf{u} - \nabla p_a}{\theta_2} \quad (33b)$$

此时, 式 (28) ~ 式 (30) 中各参数可表示为

$$B_{11m} = (\delta'_6 \delta'_8 - \delta'_5 \delta'_9) / \{[(\delta'_3 \delta'_5 - \delta'_2 \delta'_6) \delta'_7 + (\delta'_1 \delta'_6 - \delta'_3 \delta'_4) \delta'_8 + (\delta'_2 \delta'_4 - \delta'_1 \delta'_5) \delta'_9] \delta'\}$$

$$B_{12m} = (\delta'_4 \delta'_9 - \delta'_6 \delta'_7) / \{[(\delta'_3 \delta'_5 - \delta'_2 \delta'_6) \delta'_7 + (\delta'_1 \delta'_6 - \delta'_3 \delta'_4) \delta'_8 + (\delta'_2 \delta'_4 - \delta'_1 \delta'_5) \delta'_9] \delta'\}$$

$$B_{2m} = (\delta'_5 \delta'_7 - \delta'_4 \delta'_8) / \{[(\delta'_3 \delta'_5 - \delta'_2 \delta'_6) \delta'_7 + (\delta'_1 \delta'_6 - \delta'_3 \delta'_4) \delta'_8 + (\delta'_2 \delta'_4 - \delta'_1 \delta'_5) \delta'_9] \delta'\}$$

$$\delta' = \delta, \delta'_1 = \eta'_{11m} K_0(\zeta_{11m} r_0), \delta'_2 = \eta'_{12m} K_0(\zeta_{12m} r_0)$$

$$\delta'_3 = \eta'_{2m} K_0(\zeta_{2m} r_0), \delta'_4 = \delta_4, \delta'_5 = \delta_5, \delta'_6 = \delta_6$$

$$\delta'_7 = \frac{\zeta_{11m}}{\theta_1} (\varsigma_{11m} - b^1 i \omega) - \frac{\zeta_{11m}}{\theta_2} (\varsigma_{11m} - b^a i \omega)$$

$$\delta'_8 = \frac{\zeta_{12m}}{\theta_1} (\varsigma_{12m} - b^1 i \omega) - \frac{\zeta_{12m}}{\theta_2} (\varsigma_{12m} - b^a i \omega)$$

$$\delta'_9 = m\zeta_{2m} i \omega \left(\frac{b^a}{\theta_2} - \frac{b^1}{\theta_1} \right)$$

2.3 能量场特性

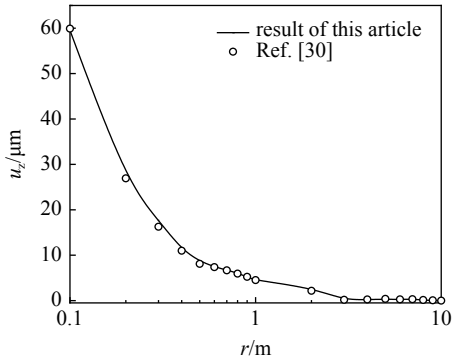
通常情况下, 半空间表面单位面积的能量传播情况可由其表面牵引力和质点运动速度的积表示^[29]. 因此, 对于本文所考虑的非饱和多孔介质材料, 单位面积上的能量, 可由式 (34) 表示, 结合两类边界条件 (1) 和 (2) 可求得不同透水 (气) 条件下, 非饱和半空间表面受到简谐荷载作用时能量的传输性质.

$$\mathbf{E}_u = \sigma_{ij} \dot{\mathbf{u}} + p_1 \dot{\mathbf{w}} + p_a \dot{\mathbf{v}} \quad (34)$$

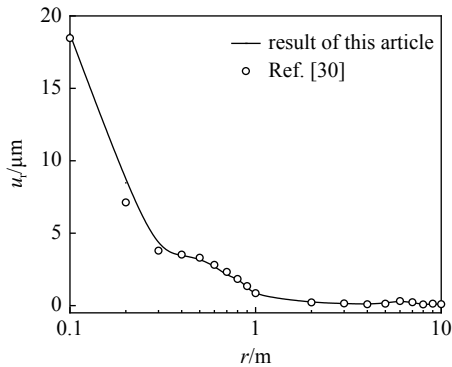
3 解答的有效性验证

在经典 Lamb 问题的分析研究中, 学者们往往

采用位移解的形式进行描述. 为验证本文计算结果的准确性, 利用式 (29) 得出的非饱和半空间表面的竖向位移 u_z 和水平位移 u_r 的解析解答, 同文献 [29] 在饱和半空间中的计算结果进行对比, 其分析结果十分接近, 说明本文所得结果可以和经典饱和半空间理论很好地衔接, 进一步证明本文计算结果的有效性, 如图 2 所示.



(a) 垂直位移
(a) Vertical displacement



(b) 水平位移
(b) Horizontal displacement

图 2 有效性验证
Fig. 2 Validity verification

4 数值分析与讨论

为讨论不同边界条件下相关参数对非饱和半空间动力响应和能量传输特性的影响规律, 本文将通过数值算例分析在不透水(气)条件、透水(气)条件下土体表面位移及能量变化受到饱和度、振动频率、渗透系数的影响情况. 数值算例中所选取的计算参数如表 1 所示.

在激振圆频率 $\omega = 1 \text{ rad/s}$ 时, 图 3 绘制了非饱和半空间表面处为不透水(气)条件、透水(气)条件时, 饱和度变化对其表面位移及能量传输特性的影响曲线. 由图 3 可见, 非饱和半空间表面位移幅值

表 1 计算参数^[17]

Table 1 Calculation parameters^[17]

Parameters	Value
λ/MPa	12.9
μ/MPa	19.4
$\rho_s/(\text{kg}\cdot\text{m}^{-3})$	2700
$\rho_l/(\text{kg}\cdot\text{m}^{-3})$	1000
$\rho_a/(\text{kg}\cdot\text{m}^{-3})$	1.29
$K_s/(\text{GPa})$	36
$K_l/(\text{GPa})$	2.0
$K_a/(\text{kPa})$	100
K/m^2	1×10^{-13}
$g/(\text{m}\cdot\text{s}^{-2})$	10
q_0/kN	1
t/s	60
$\alpha_{vg}/\text{Pa}^{-1}$	1×10^{-4}
n_{vg}	2.0
m_{vg}	0.5
n	0.6
S_r	0.6
S_{w0}	0.05
η_l	1×10^{-3}
η_a	1.8×10^{-5}

会随着饱和度的增大而增大. 这主要是由于随着饱和度的升高, 非饱和介质中基质吸力降低而引起颗粒间吸应力降低, 使半空间抵抗外力变形的能力减弱, 导致半空间表面位移幅值会呈现出逐渐增大的趋势. 在不透水(气)条件下, 整体的位移幅值低于透水(气)条件下的位移幅值, 当饱和度较低时, 孔隙内部存在大量气体, 由于气体本身有很强的可压缩性, 因此当饱和度较低时, 两种不同边界条件下的位移幅值相差很小; 当饱和度较高时, 土中孔隙水的含量明显升高, 非饱和介质抵抗变形的能力也会随之提升, 因此当饱和度较高时, 不透水(气)条件下的位移幅值会较为明显的低于透水(气)条件下的位移幅值. 同位移幅值的变化情况类似, 半空间中的能量同样呈现出随着距离振源位置的增大而振荡下降的趋势, 且当表面不透水(气)条件下, 孔隙流体压力占比相对更大, 但由于总应力没有变化, 导致有效应力占

比相对较小, 因此在不透水(气)条件下半空间表面受外荷载作用时的总能量值依然小于透水(气)条件下的能量.

以在透水(气)和不透水(气)两种不同边界条件下的位移幅值显现出一定的差异, 荷载振动频率较大时的现象与之相反. 且由于施加的外力水平不变, 因此非饱和和半空间中的能量变化会呈现出相似的变化趋势.

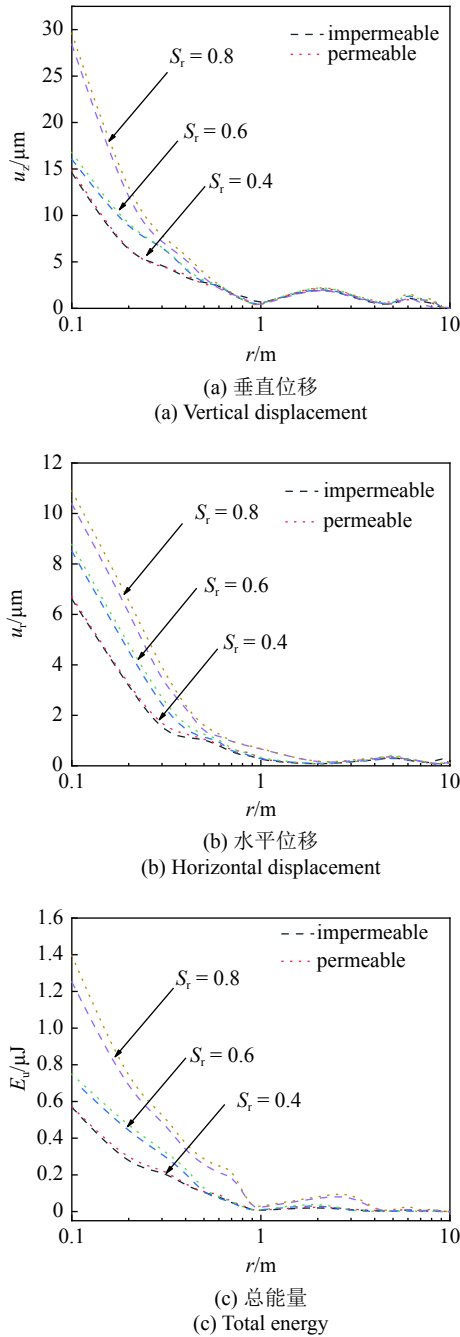


图 3 饱和度对位移和能量的影响曲线

Fig. 3 Influence curve of saturation on displacement and energy

为了分析荷载激振圆频率对非饱和半空间表面位移及能量传输特性的影响, 图 4 绘出了不同频率下相关物理量的变化曲线. 从图 4 可以看出, 随着激振频率的逐渐增加, 不论是径向还是竖向位移的幅值均逐渐减小. 因为在荷载振动频率较小时, 透水(气)条件下的地表孔隙水(气)压力更容易消散, 所

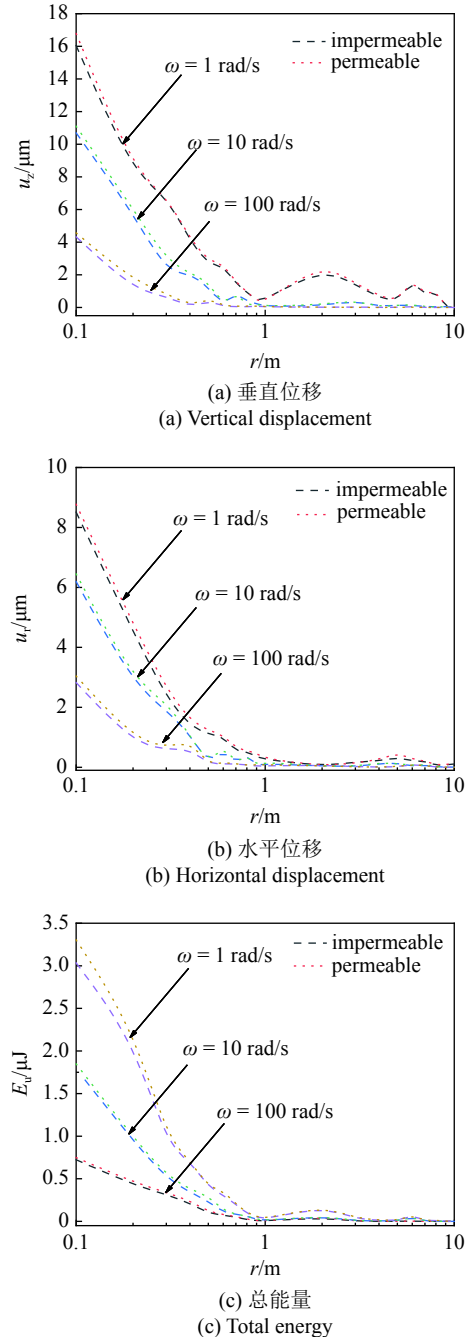


图 4 激振频率对位移和能量的影响曲线

Fig. 4 Influence curve of excitation frequency on displacement and energy

在 $\omega = 1 \text{ rad/s}$, 饱和度 $S_r = 0.6$ 时, 图 5 给出了固有渗透系数的变化对半空间表面位移幅值和能量传输特性的影响曲线. 由图 5 可见, 随着固有渗透系数

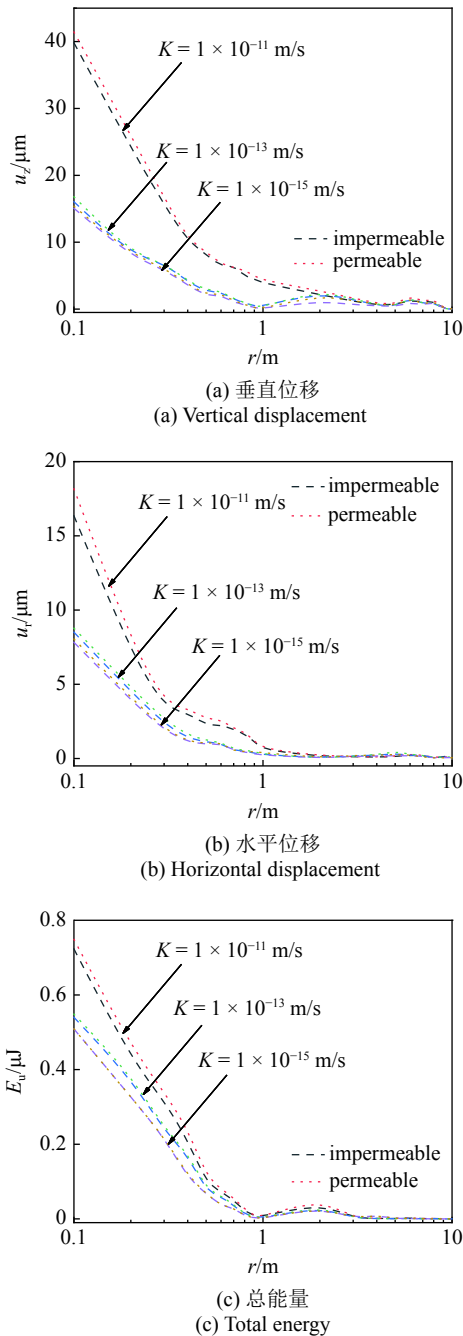


图 5 渗透系数对位移和能量的影响曲线

Fig. 5 Influence curve of permeability coefficient on displacement and energy

的逐渐降低, 骨架位移也随之减小. 随着距离振源位置的逐渐增加, 位移幅值呈现出振荡下降的现象. 当渗透系数很低时, 两种边界条件的性质趋于一致, 因为在条件 (1) 的情况下, 表面虽透水 (气), 但由于半空间内部的孔隙水 (气) 压力难以快速消散, 依然会对土骨架产生一定的支持作用, 所以位移幅值会随着渗透系数的降低而呈现出一定的下降趋势. 在不透水 (气) 条件下, 孔隙流体会持续影响半空间的表

面位移, 且孔隙中流体和土骨架之间没有相对位移, 因此不透水 (气) 边界条件下非饱和半空间表面的位移幅值会略低于透水 (气) 边界条件下的位移幅值, 且当土骨架位移幅值减小时, 总能量也会呈现出减小的现象, 当渗透系数下降至 $K < 1 \times 10^{-13}$ m/s 时, 地表位移幅值受渗透系数影响趋于一极限值, 并且随着渗透系数的逐渐降低, 这两种不同边界条件所产生的宏观现象会逐渐趋于一致, 但其差异性将一直存在.

5 结论

采用 Helmholtz 分解法, 给出了垂直集中简谐荷载作用下的非饱和土的动力响应解答, 并通过数值算例分析了荷载振动频率、饱和度、渗透系数以及孔隙率对非饱和半空间位移场和能量场的影响规律. 所得结论如下:

(1) 激振频率对非饱和半空间表面的动力响应和能量传输特性有着显著的影响, 随着激振频率逐渐增大, 表面位移幅值及总体能量水平平均逐渐减小, 且随着距离振源位置的逐渐增加, 位移幅值呈现出振荡减小的现象, 渗透系数越高, 激振频率越小, 该现象越明显.

(2) 表面位移幅值随着饱和度的减小而降低, 并且降低渗透系数也同样会减小位移幅值, 当渗透系数的降低到一定程度时, 位移幅值下降速度放缓, 并逐渐趋于一个极限值.

参 考 文 献

- 1 Biot MA. Theory of propagation of elastic waves in a fluid-saturated porous solid, part I: low-frequency range. *The Journal of the Acoustical Society of America*, 1956, 28(2): 168-178
- 2 Biot MA. Theory of propagation of elastic waves in a fluid-saturated porous solid part II: higher-frequency range. *The Journal of the Acoustical Society of America*, 1956, 28(2): 179-191
- 3 雷晓燕, 徐斌, 徐满清. 半无限弹性空间中移动荷载动力响应的频域-波数域比例边界有限元法分析. *振动工程学报*, 2017, 30(5): 798-805 (Lei Xiaoyan, Xu Bin, Xu Manqing. Using the frequency-wave domain scaled boundary finite element method for the dynamic response of the elastic half space due to moving loads. *Journal of Vibration Engineering*, 2017, 30(5): 798-805 (in Chinese))
- 4 王立安, 赵建昌, 侯小强等. 非均匀饱和半空间的 Lamb 问题. *岩土力学*, 2020, 41(5): 1790-1798 (Wang Lian, Zhao Jianchang, Hou Xiaoqiang. Lamb problem for non-homogeneous saturated half-space. *Rock and Soil Mechanics*, 2020, 41(5): 1790-1798 (in Chinese))
- 5 Bo J, Huati L. Vertical dynamic response of a disk on a saturated

- poroelastic half-space. *Soil Dynamics & Earthquake Engineering*, 1999, 18(6): 437-443
- 6 邹新军, 贺琼, 覃玉兰. 竖向非均质饱和地基中埋置扭转荷载的动力响应. 湖南大学学报(自然科学版), 2020, 47(3): 11-18 (Zou Xinjun, He Qiong, Qin Yulan. Dynamic response of buried torsional load in vertically non-homogeneous saturated soil. *Journal of Hunan University (Natural Sciences)*, 2020, 47(3): 11-18 (in Chinese))
 - 7 Wu M. Three-dimensional dynamic Green's functions for transversely isotropic saturated half-space subjected to buried loads. *Engineering Analysis with Boundary Elements*, 2019, 108: 301-320
 - 8 Li YC, Feng SJ, Chen HX, et al. Dynamic response of a stratified transversely isotropic half-space with a poroelastic interlayer due to a buried moving source. *Applied Mathematical Modelling*, 2020, 82: 45-71
 - 9 Gakenheimer DC. Numerical results for Lamb's point load problem. *Journal of Applied Mechanics*, 1970, 37(2): 522-524
 - 10 Han B, Liang JW, Fu J, et al. 3D dynamic soil-structure interaction in layered, fluid-saturated, poroelastic half-space - ScienceDirect. *Soil Dynamics and Earthquake Engineering*, 2019, 120: 113-126
 - 11 Zhang ZQ, Pan E. Vertical vibration of a rigid circular disc embedded in a transversely isotropic and layered poroelastic half-space. *Engineering Analysis with Boundary Elements*, 2020, 118: 84-95
 - 12 Ba ZN, Wu MT, Liang JW. 3D dynamic responses of a multi-layered transversely isotropic saturated half-space under concentrated forces and pore pressure. *Applied Mathematical Modelling*, 2020, 80: 859-878
 - 13 Ai ZY, Li Y, Liu CL. Behavior of a multilayered transversely isotropic half space due to horizontal transient loadings. *Computers and Geotechnics*, 2018, 97: 217-221
 - 14 时刚, 高广运, 郭院成. 饱和层状地基的瞬态动力响应分析. 郑州大学学报(工学版), 2010, 31(2): 52-55 (Shi Gang, Gao Guangyun, Guo Yuan Cheng. Analysis of Transient Response of Saturated Layered Half-space Soli. *Journal of Zhengzhou University(Engineering Science)*, 2010, 31(2): 52-55 (in Chinese))
 - 15 王春玲, 赵鲁珂, 李东波. 非饱和地基上多层矩形板稳态响应解析研究. 岩土工程学报, 2019, 41(12): 2182-2190 (Wang Chunling, Zhao Luke, Li Dongbo. Analytical study on dynamic response of multi-layered plate in unsaturated half-space. *Rock and Soil Mechanics*, 2019, 41(12): 2182-2190 (in Chinese))
 - 16 王春玲, 赵鲁珂. 成层非饱和地基上矩形基础稳态响应解析研究. 应用力学学报, 2020, 37(3): 1131-1137 (Wang Chunling, Zhao Luke. Analytical study on steady-state response of rectangular foundation on layered unsaturated subgrade. *Chinese Journal of Applied Mechanics*, 2020, 37(3): 1131-1137 (in Chinese))
 - 17 王春玲, 赵鲁珂, 刘韡. 混合边界约束多层矩形薄板的自由振动解析研究. 应用力学学报, 2020, 37(1): 390-396 (Wang Chunling, Zhao Luke, Liu Wei. Analytical study of free vibration for layered rectangular plate with mixed boundary conditions. *Chinese Journal of Applied Mechanics*, 2020, 37(1): 390-396 (in Chinese))
 - 18 徐明江. 非饱和土地基与基础的动力响应研究. [博士论文]. 广州: 华南理工大学, 2010 Xu Mingjiang. Investigation on dynamic responses of unsaturated soils and foundation. [PhD Thesis]. Guangzhou: South China University of Technology, 2010 (in Chinese)
 - 19 Xu MJ, Wei DM. 3D dynamic response of layered unsaturated soils to harmonic loads. *Journal of Donghua University (English Edition)*, 2010, 27(03): 407-411
 - 20 徐明江, 魏德敏. 非饱和多孔介质中弹性波的传播特性. 科学技术与工程, 2009, 9(18): 5403-5409 (Xu Mingjiang, Wei Demin. Characteristics of wave propagation in partially saturated poroelastic media. *Science Technology and Engineering*, 2009, 9(18): 5403-5409 (in Chinese))
 - 21 Zhang M, Wang XH, Yang GC. Solution of dynamic Green's function for unsaturated soil under internal excitation. *Soil Dynamics and Earthquake Engineering*, 2014, 64: 63-84
 - 22 Bishop AW. The effective stress principle. *Teknisk Ukeblad*, 1959, 39: 859-863
 - 23 Fredlund DG, Morgenstern NR. Stress state variables for unsaturated soils. *Journal of the Geotechnical Engineering Division ASCE*, 1977, 103(5): 447-466
 - 24 Lu N. Is matric suction a stress variable? *Journal of Geotechnical & Geoenvironmental Engineering*, 2008, 134(7): 899-905
 - 25 Lu N, Godt JW, Wu DT. A closed-form equation for effective stress in unsaturated soil. *Water Resources Research*, 2010, 46(5): 567-573
 - 26 Wei CL, Sposito G, Majer E. Immiscible two-phase fluid flows in deformable porous media. *Advances in Water Resources*, 2002, 25(8): 1105-1117
 - 27 Vardoulakis I, Beskos DE. Dynamic behavior of nearly saturated porous media. *Mechanics of Materials*, 1986, 5(1): 87-108
 - 28 Gray WG. Thermodynamics and constitutive theory for multiphase porous-media flow considering internal geometric constraints. *Advances in Water Resources*, 1999, 22(5): 521-547
 - 29 Chen WY, Chen GX, Xia TD, et al. Energy flux characteristics of seismic waves at the interface between soil layers with different saturations. *Science China Technological Sciences*, 2014, 57(10): 2062-2069
 - 30 陈龙珠, 陈胜立, 梁发云. 饱和地基竖向振动的衰减特性. 上海交通大学学报, 2002, 36(3): 376-381 (Chen Longzhu, Chen Shengli, Liang Fayun. Vibration attenuation of saturated strata by vertical surface loads. *Journal of Shanghai Jiaotong University*, 2002, 36(3): 376-381 (in Chinese))
 - 31 van Genuchten M Th. A closed-form equation for predicting the hydraulic conductivity of unsaturated soils. *Soil Science Society of America Journal*, 1980, 44(5): 892-898

附录 A

$$a_{11} = \frac{A_{22}A_{33}}{A_{11}A_{22} - A_{12}A_{21}}, a_{12} = \frac{A_{22}A_{14} - A_{12}A_{24}}{A_{11}A_{22} - A_{12}A_{21}}$$

$$a_{13} = \frac{A_{22}A_{15} - A_{12}A_{25}}{A_{11}A_{22} - A_{12}A_{21}}, a_{21} = -\frac{A_{21}A_{13}}{A_{11}A_{22} - A_{12}A_{21}}$$

$$a_{22} = -\frac{A_{11}A_{24} - A_{21}A_{14}}{A_{11}A_{22} - A_{12}A_{21}}, a_{23} = \frac{A_{11}A_{25} - A_{21}A_{15}}{A_{11}A_{22} - A_{12}A_{21}}$$

$$A_{11} = \frac{\alpha S_e - nS_r}{K_s} + \frac{nS_r}{K_1}$$

$$A_{12} = \frac{\alpha(1 - S_e) - n(1 - S_r)}{K_s} + \frac{n(1 - S_r)}{K_a}$$

$$A_{13} = 1 - n - \frac{K_a}{K_s}, A_{14} = nS_r, A_{15} = n(1 - S_r)$$

$$A_{21} = A_s - \frac{S_r(1-S_r)}{K_l}, A_{22} = \frac{S_r(1-S_r)}{K_a} - A_s$$

$$A_{24} = -A_{25} = -S_r(1-S_r)$$

$$A_s = -\alpha_{vg} m_{vg} n_{vg} (1-S_{w0}) S_e^{\frac{m_{vg}+1}{m_{vg}}} \left(S_e^{-\frac{1}{m_{vg}}} - 1 \right)^{\frac{n_{vg}-1}{n_{vg}}}$$

附录 B

考虑土颗粒由于粒间吸应力所引起的变形为

$$\varepsilon_{11}^s = \varepsilon_{22}^s = \varepsilon_{33}^s = -\frac{\sigma_s}{3K_s} \quad (B1)$$

则结合有效应力公式 (5), 弹性本构关系可表示为

$$\sigma'_{ij} = \lambda e \delta_{ij} + 2\mu \varepsilon_{ij} + \frac{K_b}{K_s} (\sigma_s + p_a) \delta_{ij} \quad (B2)$$

式中, $e = \frac{\partial u_r}{\partial r} + \frac{u_r}{r} + \frac{1}{r} \frac{\partial u_\theta}{\partial \theta} + \frac{\partial u_z}{\partial z}$, 表示土骨架的体应变. 令 $\alpha = 1 - K_b/K_s$, 将有效应力公式 (5) 代入式 (B2), 整理后即可得到本构方程 (7).

附录 C

根据平均化方法, 总应力又可表示为

$$\sigma_{ij} = (1-n)\sigma'_{ij} - nS_r p_l \delta_{ij} - n(1-S_r) p_a \delta_{ij} \quad (C1)$$

由式 (B2) 和式 (C1) 联立得

$$\sigma'_{ij} = \frac{1}{1-n} \left\{ \lambda e \delta_{ij} + 2\mu \varepsilon_{ij} - (\alpha S_e - nS_r) p_l \delta_{ij} - [\alpha(1-S_e) - n(1-S_r)] p_a \delta_{ij} \right\} \quad (C2)$$

由粒间应力所引起的土颗粒的密度变化为

$$\frac{d\rho_s}{\rho_s dt} = -\frac{de}{dt} = -\frac{d\sigma'_{ij}}{3K_s dt} \quad (C3)$$

由式 (C2) 和式 (C3) 得

$$\frac{d\rho_s}{\rho_s dt} = \frac{1}{(1-n)K_s} \{ -K_b \nabla \cdot \dot{u} + (\alpha S_e - nS_r) \dot{p}_l + [\alpha(1-S_e) - n(1-S_r)] \dot{p}_a \} \quad (C4)$$

同理, 对于液相和气相的变化也有类似的关系

$$\frac{d\rho_l}{\rho_l dt} = \frac{dp_l}{K_l dt}, \frac{d\rho_a}{\rho_a dt} = \frac{dp_a}{K_a dt} \quad (C5)$$

将式 (15) 进一步展开得到更详细的表达形式

$$-\dot{n}\rho_s + (1-n)\dot{\rho}_s + (1-n)\rho_s \nabla \cdot \dot{u} - \rho_s \dot{u} \cdot \nabla n + (1-n)\dot{u} \cdot \nabla \rho_s = 0 \quad (C6a)$$

$$n\rho_l \dot{S}_r + S_r \rho_l \dot{n} + S_r n \dot{\rho}_l + nS_r \rho_l \nabla \cdot \dot{w} + S_r \rho_l \dot{w} \cdot \nabla n + n\rho_l \dot{w} \cdot \nabla S_r + nS_r \dot{w} \cdot \nabla \rho_l = 0 \quad (C6b)$$

$$-n\rho_a \dot{S}_r + (1-S_r)\rho_a \dot{n} + (1-S_r)n\dot{\rho}_a + (1-S_r)n\rho_a \nabla \cdot \dot{v} - n\rho_a \dot{v} \cdot \nabla S_r + (1-S_r)\rho_a \dot{v} \cdot \nabla n + (1-S_r)n\dot{v} \cdot \nabla \rho_a = 0 \quad (C6c)$$

通常情况下因变量的空间导数与时间导数的积与时间导数相比, 空间导数与时间导数的积是高阶小量, 因此式 (C6a) ~ (C6c) 可以简化写成

$$-\dot{n} + (1-n)\frac{\dot{\rho}_s}{\rho_s} + (1-n)\nabla \cdot \dot{u} = 0 \quad (C7a)$$

$$n\dot{S}_r + \dot{n}S_r + nS_r \frac{\dot{\rho}_l}{\rho_l} + nS_r \nabla \cdot \dot{w} = 0 \quad (C7b)$$

$$-n\dot{S}_r + \dot{n}(1-S_r) + n(1-S_r)\frac{\dot{\rho}_a}{\rho_a} + n(1-S_r)\nabla \cdot \dot{v} = 0 \quad (C7c)$$

将式 (C4) 代入式 (C7a) 得

$$\dot{n} = \left(1-n - \frac{K_b}{K_s} \right) \nabla \cdot \dot{u} + \frac{\alpha S_e - nS_r}{K_s} \dot{p}_l + \frac{\alpha(1-S_e) - n(1-S_r)}{K_s} \dot{p}_a \quad (C8)$$

根据 van Genuchten 提出的水土特征曲线^[31] 饱和度 S_r 相对时间的导数可以写成

$$\dot{S}_r = -\alpha_{vg} m_{vg} n_{vg} (1-S_{w0}) S_e^{\frac{m_{vg}+1}{m_{vg}}} \cdot \left(S_e^{-\frac{1}{m_{vg}}} - 1 \right)^{\frac{n_{vg}-1}{n_{vg}}} (\dot{p}_a - \dot{p}_l) \quad (C9)$$

式中, $\alpha_{vg}, m_{vg}, n_{vg}$ 分别为 V-G 模型下表征水土特征的拟合参数; S_r 为土体饱和度.

将式 (C5)、式 (C8)、式 (C9) 代入式 (C7b) 和式 (C7c), 整理后可得到非饱和土中的渗流连续方程 (8).